Ref. Ares(2025)1616772 - 28/02/2025

EASI SMR

D7.2 Specifications of LDR-50 fresh core at BOC conditions

Ville Valtavirta, Riku Tuominen
(VTT)

1. Document information

Grant Agreement Number	n°101164810
Project Title	Ensuring Assessment of Safety Innovations for SMR
Project Acronym	EASI-SMR
Project Coordinator	Nicolas Sobecki
Project Duration	1 September 2024 – 31 August 2028 (48 months)
Related Work Package	WP7 Advanced Core Physics Studies of Boron-Free SMR-cores
Lead Organisation	VTT
Contributing Partner(s)	-
Submission Date	28.02.2025
Dissemination Level	Public

2. History

Date	Submitted by	Reviewed by	Version (Notes)
05.02.2025	V. Valtavirta (VTT)		Initial release
12.02.2025		V.-H. Sanchez-Espinoza	
13.02.2025	V. Valtavirta (VTT)		Revision, accept changes from review.
20.02.2025		N. Sobecki	
25.02.2025	V. Valtavirta (VTT)		Revision V2, adjustments based on review.

Co-funded by the European Union
UK Research and Innovation
The Research Council of Norway
Project funded by

Table of Contents

List of Figures

List of Tables

Co-funded by the European Union
UK Research and Innovation
The Research Council of Norway
Project funded by

3. Summary

This deliverable gives the specifications for the LDR lite core model at the beginning of the initial cycle and also provides the fuel reloading strategy used to reach the equilibrium cycle. This forms the basis of the LDR lite related analysis work conducted in Work Package 7 continuing now with the construction of the beginning of cycle core calculation models by the partners and their verification with comparison studies in Subtask 7.2.2.

The geometry and material specifications of this document as well as the core level boundary conditions and the reloading map will be utilized throughout the analysis work and will be accompanied by specific calculation scenario definitions as needed for the initial verification (Subtask 7.2.2), transient analysis (Subtask 7.3.2) and equilibrium cycle simulation (Subtask 7.5.2).

4. Keywords

LDR-50, LDR lite, benchmark, core design

5. Abbreviations and acronyms

Acronym	Description
BOC	Beginning of Cycle
CR	Control Rod
LDR	Low temperature District heating Reactor
SG	Spacer Grid
WP	Work Package

Co-funded by the European Union
UK Research and Innovation
The Research Council of Norway
Project funded by

6. Introduction

The LDR lite benchmark is modelled in WP7 of the EASI-SMR as a public representation of the LDR-50 small modular reactor concept, initially developed at VTT Technical Research Centre of Finland Ltd and currently being commercialized by Steady Energy Oy. The LDR-50 is a low temperature and low pressure light water reactor concept designed for low temperature heat production for applications such as district heating. As the reactor is not aimed for electricity production, the temperatures and pressures in the primary circuit can be kept at low levels. The reactor includes in-vessel control rod drives, self-pressurization, natural circulation in the primary circuit and boron free operation.

This document describes the LDR lite core at a level sufficient for creating models for core-level neutronics, thermal hydraulics and fuel behaviour solvers. The system scale effects are not included in these specifications. The description is heavily based on the public LDR lite specification (Komu & Tuominen, 2025), but has been edited here to include only those parts relevant for the core modelling.

The verification of the created models at the beginning of initial cycle will be conducted among partners in Subtask 7.2.2 using specific benchmark tasks determined at that point. After that, the multi-physics core level transient analyses for the beginning of the cycle state can be conducted in Subtask 7.3.2 and reported in Deliverable 7.6. Equilibrium cycle simulation will be performed in Subtask 7.5.2, starting from the initial core and based on the reloading strategy defined in this document and the equilibrium core state, thus obtained, will be utilized again in Subtask 7.3.2 in modelling the transients at the equilibrium cycle state (Deliverable 7.8).

7. Radial geometry

7.1. Overview

The reactor core consists of 37 square fuel assemblies (17x17 type) surrounded by a stainless steel reflector. The radial geometry of the reactor core model is presented in Figure 1. The stainless steel reflector is surrounded by a water cylinder representing the downcomer. The fuel is low enriched UO_2 and some of the assemblies contain fuel rods with gadolinium as a burnable absorber. The core loading pattern for the initial core is shown in Figure 2. In total there are six different assembly types in the initial core. General fuel assembly parameters are presented in Table 1 and key properties of the assembly types in Table 2.

Co-funded by the European Union
UK Research and Innovation
The Research Council of Norway
Project funded by

Table 1. General fuel assembly parameters.

Parameter	Value
Fuel assembly lattice pitch	21.50364 cm
Pin lattice pitch	1.25984 cm
Pin lattice configuration	17x17
Number of fuel rods	264
Number of guide tubes	24
Number of instrumentation tubes	1

Table 2. Key properties of the assembly types.

Assembly type	1	2	3	4	5	6
^{235}U enrichment (wt-%)	1.5	1.4	1.8	2.4	2.4	1.8
Number of Gd rods	8	-	4	8	8	-
Gd_2O_3 content (wt-%)	6.0	-	6.0	5.0	9.0	-
Uranium mass (g)	125987	126217	126102	126024	125871	126216

Co-funded by the European Union
UK Research and Innovation
The Research Council of Norway
Project funded by

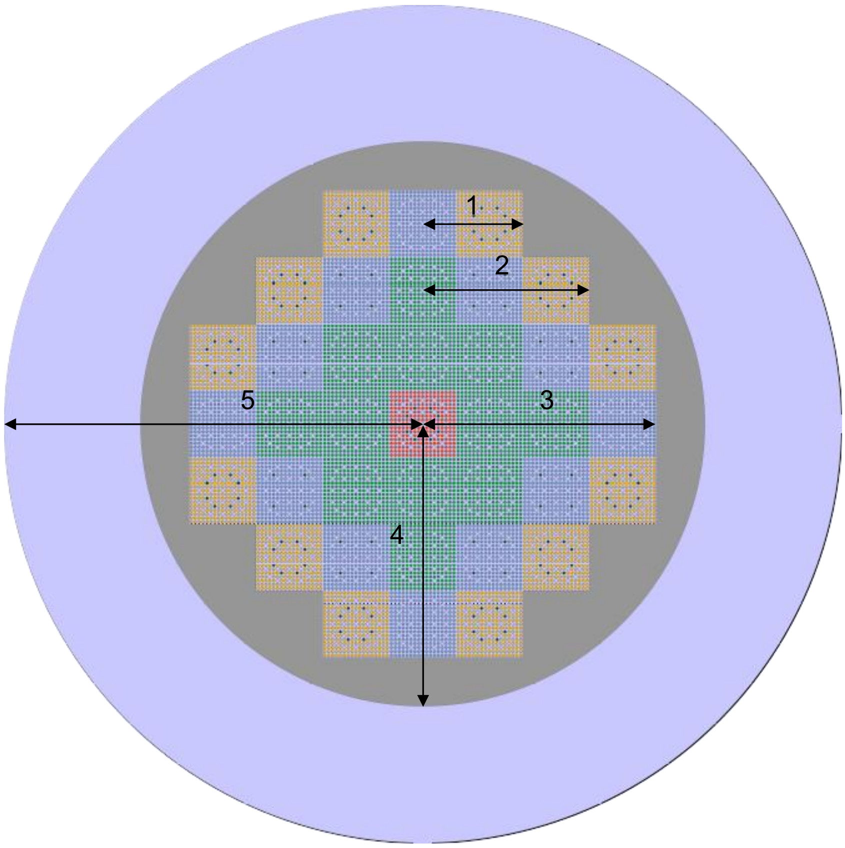

Dimension	Description	Length (cm)
1	Radial reflector inner boundary	32.25546
2	Radial reflector inner boundary	53.75910
3	Radial reflector inner boundary	75.26274
4	Radial reflector outer boundary	91.00000
5	Outer boundary of the model	135.0000

Figure 1. Radial geometry of the reactor core model.

Co-funded by the European Union
UK Research and Innovation
The Research Council of Norway
Project funded by

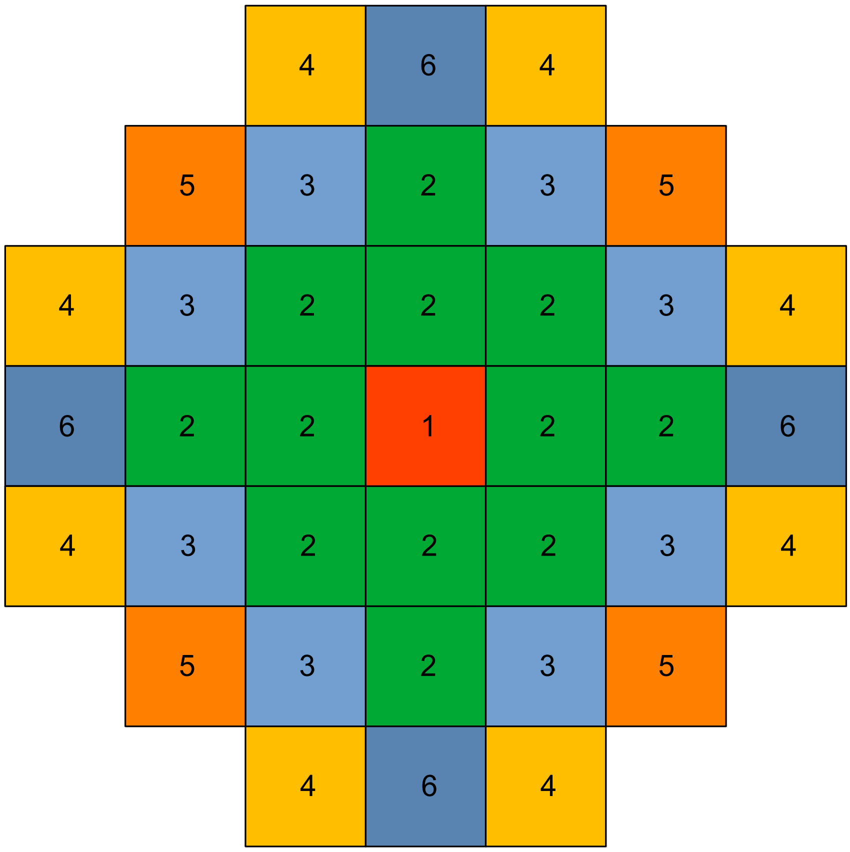

Assembly type	Description
1	1.50 wt-% ^{235}U, 8 rods with 6.00 wt-% Gd_2O_3
2	1.40 wt-% ^{235}U
3	1.80 wt-% ^{235}U, 4 rods with 6.00 wt-% Gd_2O_3
4	2.40 wt-% ^{235}U, 8 rods with 5.00 wt-% Gd_2O_3
5	2.40 wt-% ^{235}U, 8 rods with 9.00 wt-% Gd_2O_3
6	1.80 wt-% ^{235}U

Figure 2. Core loading pattern for the initial core.

Co-funded by the European Union
UK Research and Innovation
The Research Council of Norway
Project funded by

7.2. Control rod groups

Control rod groups are present in each assembly, and they are divided into 8 groups with 4 regulating groups and 4 safety groups. The locations of the groups are shown in Figure 3.

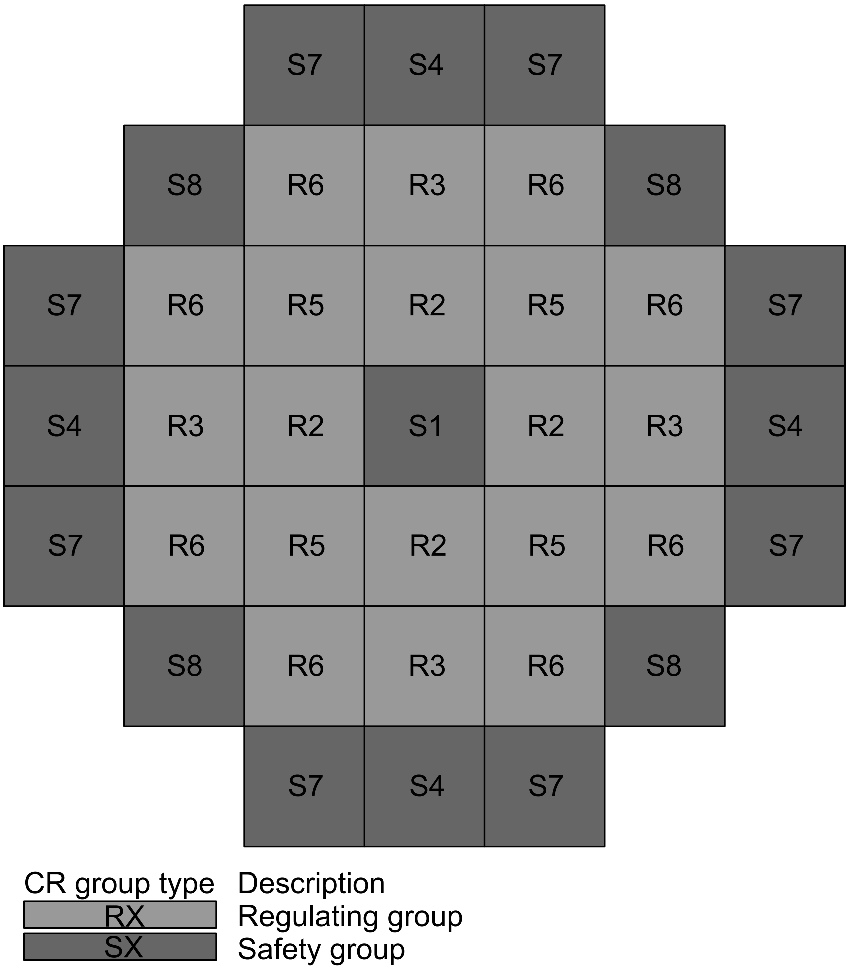

Figure 3. Locations of the control rod groups.

Co-funded by the European Union
UK Research and Innovation
The Research Council of Norway
Project funded by

7.3. Assembly layouts

The locations of the 8 gadolinium fuel rods in assembly types 1, 4 and 5 are presented in Figure 4 and the locations of the 4 gadolinium fuel rods in assembly type 3 in Figure 5.

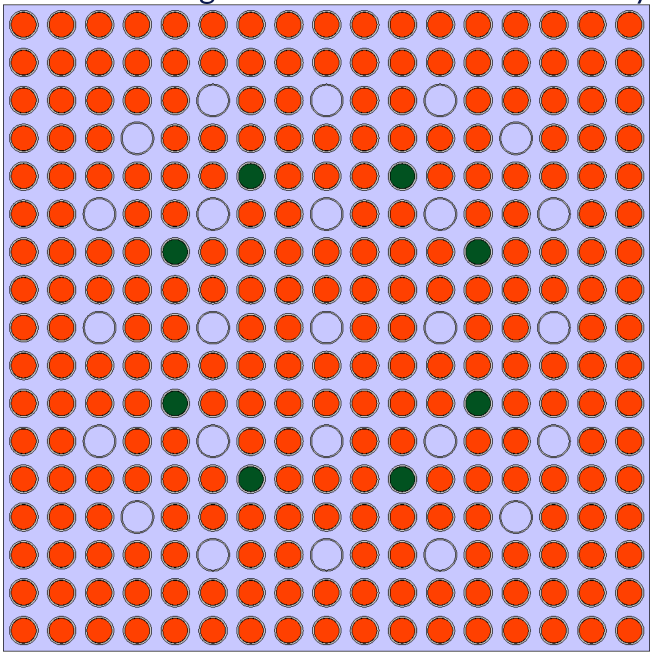

Figure 4. Layout of the fuel assembly types 1, 4 and 5 with fuel containing gadolinium shown in dark green. The water-filled empty tubes are the control rod guide tubes and the central instrumentation tube.

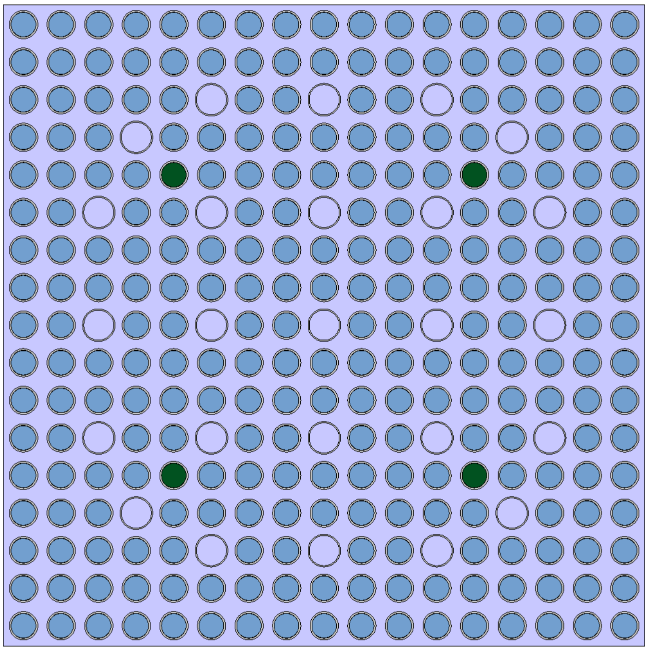

Figure 5. Layout of the fuel assembly type 3 with fuel containing gadolinium shown in dark green. The water-filled empty tubes are the control rod guide tubes and the central instrumentation tube.

Co-funded by the European Union
UK Research and Innovation
The Research Council of Norway
Project funded by

7.4. Pin types

The fuel assemblies are constructed using the pin cell types defined in this section. The pin cells are surrounded by coolant.

7.4.1. Fuel rods

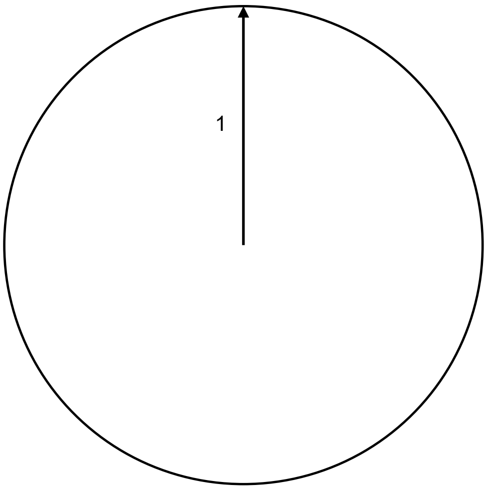

Arrow	Material	Radius (cm)
1	Steel	0.30967

Figure 6: Steel pin for the support plate/nozzle regions.

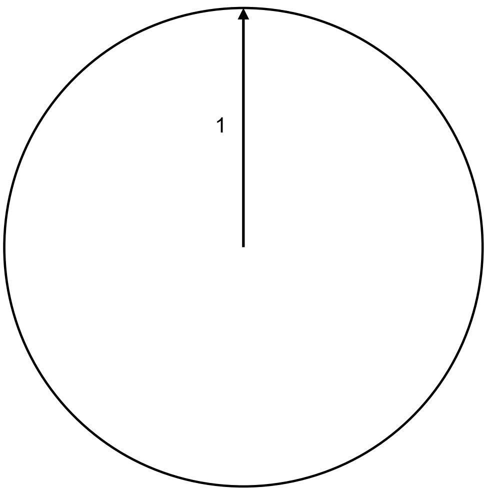

Arrow	Material	Radius (cm)
1	Zircaloy	0.47500

Figure 7. Zircaloy-4 plug for the fuel rods.

Co-funded by the European Union
UK Research and Innovation
The Research Council of Norway
Project funded by

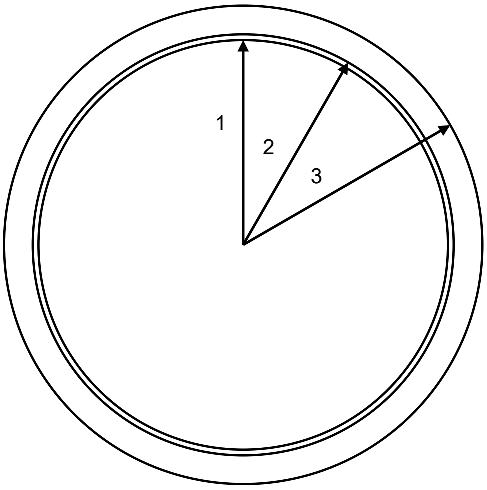

Arrow	Material	Radius (cm)
1	Fuel	0.40950
2	Helium	0.41790
3	Zircaloy	0.47500

Figure 8. Fuel pin.

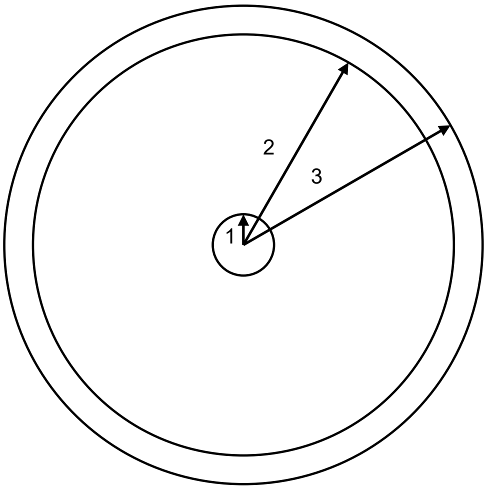

Arrow	Material	Radius (cm)
1	Steel	0.06459
2	Helium	0.41790
3	Zircaloy	0.47500

Figure 9. Fuel rod plenum.

Co-funded by the European Union
UK Research and Innovation
The Research Council of Norway
Project funded by

7.4.2. Guide tubes, instrumentation tubes and control rods

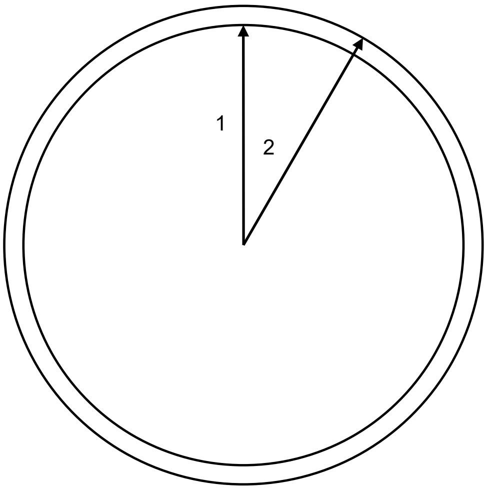

Arrow	Material	Radius (cm)
1	Coolant	0.50419
2	Zircaloy	0.54610

Figure 10. Empty guide tube/instrumentation tube.

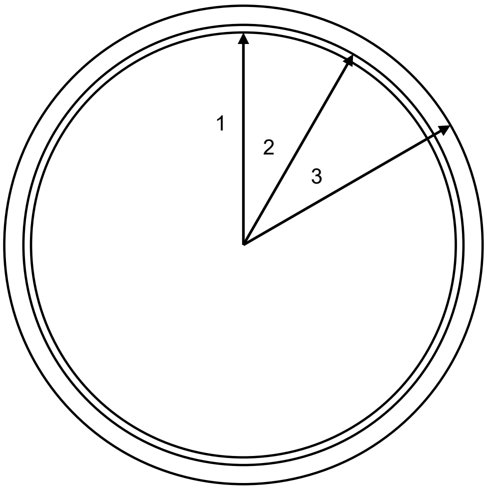

Arrow	Material	Radius (cm)
1	Steel	0.48387
2	Coolant	0.50419
3	Zircaloy	0.54610

Figure 11. Control rod steel upper part above absorber sections.

Co-funded by the European Union
UK Research and Innovation
The Research Council of Norway
Project funded by

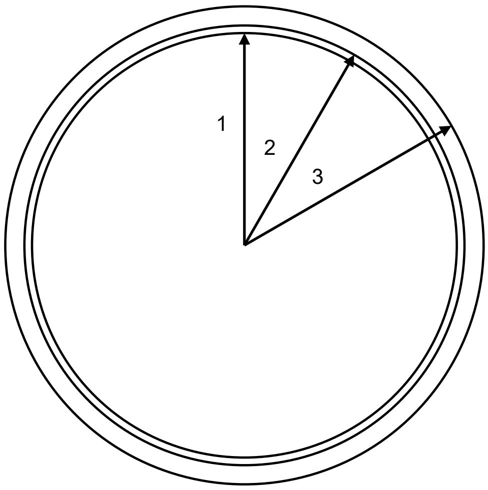

Arrow	Material	Radius (cm)
1	Inconel	0.48387
2	Coolant	0.50419
3	Zircaloy	0.54610

Figure 12. Control rod lower absorber section.

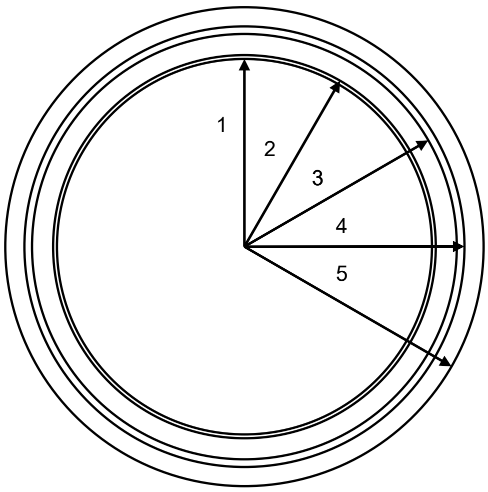

Arrow	Material	Radius (cm)
1	B4C	0.43310
2	Helium	0.43688
3	Steel	0.48387
4	Coolant	0.50419
5	Zircaloy	0.54610

Figure 13. Control rod upper absorber section.

7.5. Spacer grids

The reactor core has 3 spacer grids located at the bottom, middle and top of the active fuel region. The spacer grids are modelled using square egg-crates surrounding each pin cell in the assembly lattices and boxes for the spacer grid sleeves surrounding each assembly. Dimensions of these structures have been obtained from the BEAVRS

Co-funded by the European Union
UK Research and Innovation
The Research Council of Norway
Project funded by
Schweizerische Eidgenossenschaft Confédération suisse Confederazione Svizzera Confederaziun svizra
Swiss Confederation
Federal Department of Economic Affairs, Education and Research EAER
State Secretariat for Education, Research and Innovation SERI

benchmark (Horelik, Herman, Forget, & Smith, 2013). The bottom and the middle spacer consist entirely of Zircaloy while the top spacer has a stainless steel sleeve and Inconel-718 inner egg-crates. The height of the Zircaloy spacers is 5.715 cm and the height of the Inconel spacer is 3.358 cm. The dimensions of the Zircaloy egg-crate are shown in Figure 14 and the dimensions of the Inconel egg-crate in Figure 15. Figure 16 shows the dimensions of the grid sleeves. These dimensions are the same for all spacers. A radial view of the top spacer illustrating the egg-crates and the box structures is shown in Figure 17.

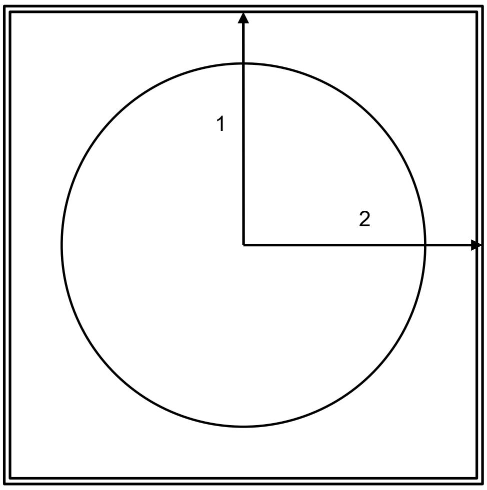

Arrow	Material	Radius (cm)
1	Coolant	0.61049
2	Zircaloy	0.62992

Figure 14. Zircaloy egg-grate surrounding each pin in the bottom and middle spacers.

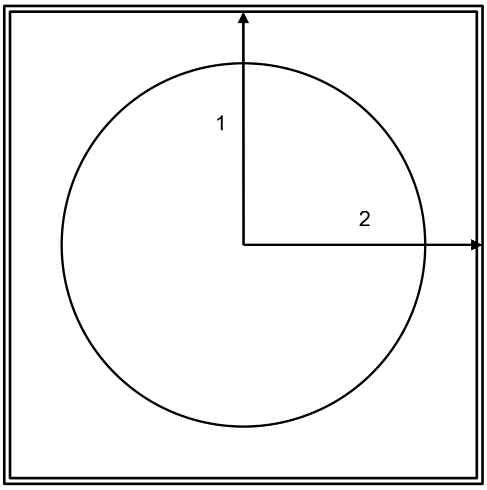

Arrow	Material	Radius (cm)
1	Coolant	0.61015
2	Inconel	0.62992

Figure 15. Inconel egg-grate surrounding each pin in the top spacer.

Co-funded by the European Union
UK Research and Innovation
The Research Council of Norway
Project funded by

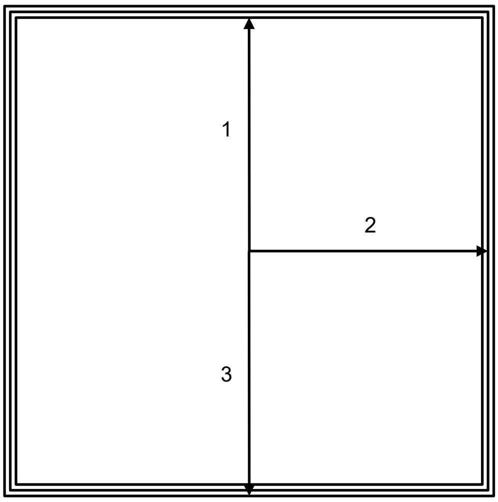

Arrow	Material	Radius (cm)
1	Assembly	10.70864
2	Steel/Zircaloy	10.74798
3	Coolant	10.75182

Figure 16. Spacer grid sleeve surrounding each assembly in the spacers.

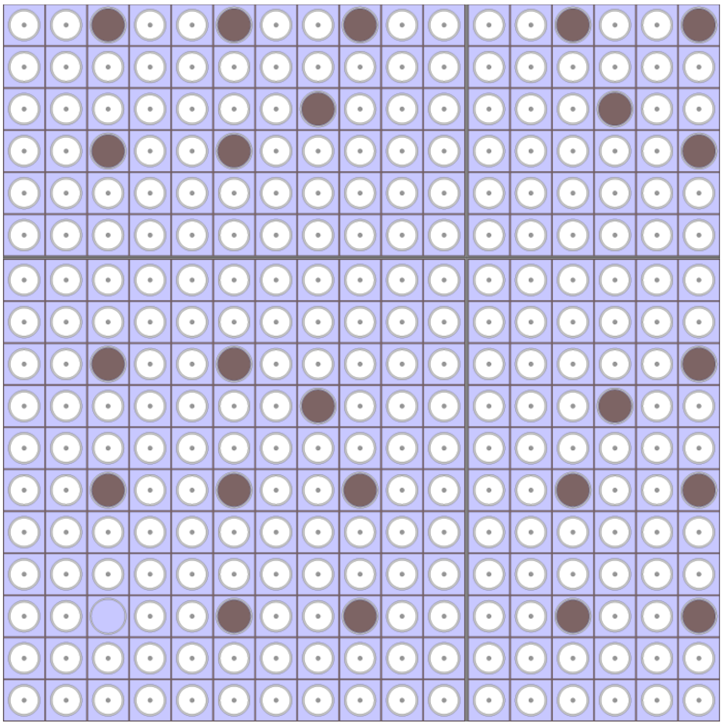

Figure 17. Radial view of the top spacer grid.

Co-funded by the European Union
UK Research and Innovation
The Research Council of Norway
Project funded by

7.6. Support plate/nozzle regions

The support plate/bottom nozzle and the top nozzle regions are approximated by stainless steel pins as shown in Figure 18. There is a steel pin at each fuel rod position. The pin radius, which is given in Figure 6, has been calculated so that the volume fraction of steel in these regions is the same as the one used in the BEAVRS benchmark. The heights of the regions have been also taken directly from BEAVRS. No distinction is made between the support plate and the bottom nozzle and they are represented by a single region.

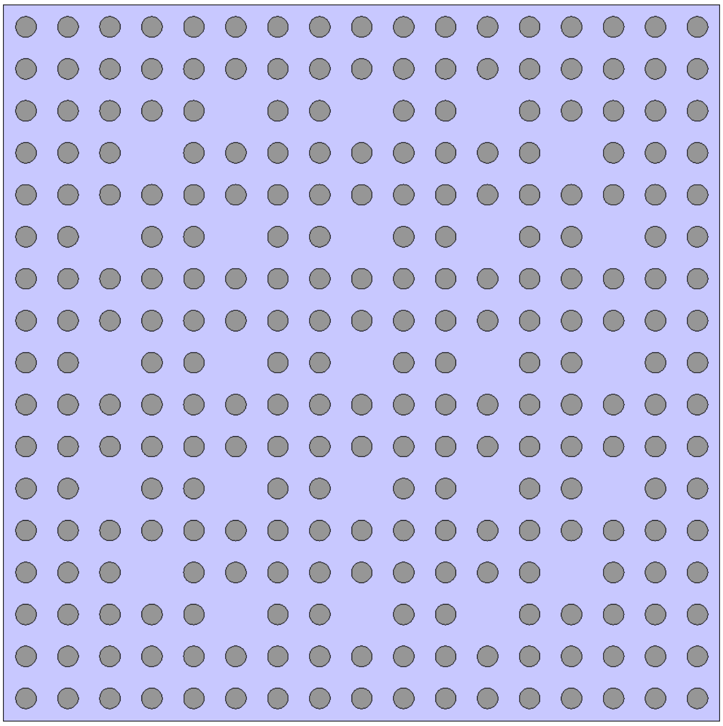

Figure 18. Radial view of the support plate/nozzle regions for one fuel assembly.

8.Axial geometry

8.1. Overview

The axial geometry of the model is illustrated in Figure 19 and in Figure 20. In the latter the axial planes needed for the construction of the geometry are given. The model is limited between the bottom of the support plate and the top of the top nozzle. Active height of the fuel is 100 cm and the total height of the model is 135.467 cm. The downcomer and reflector regions extend from the bottom to the top of the geometry.

Co-funded by the European Union
UK Research and Innovation
The Research Council of Norway
Project funded by

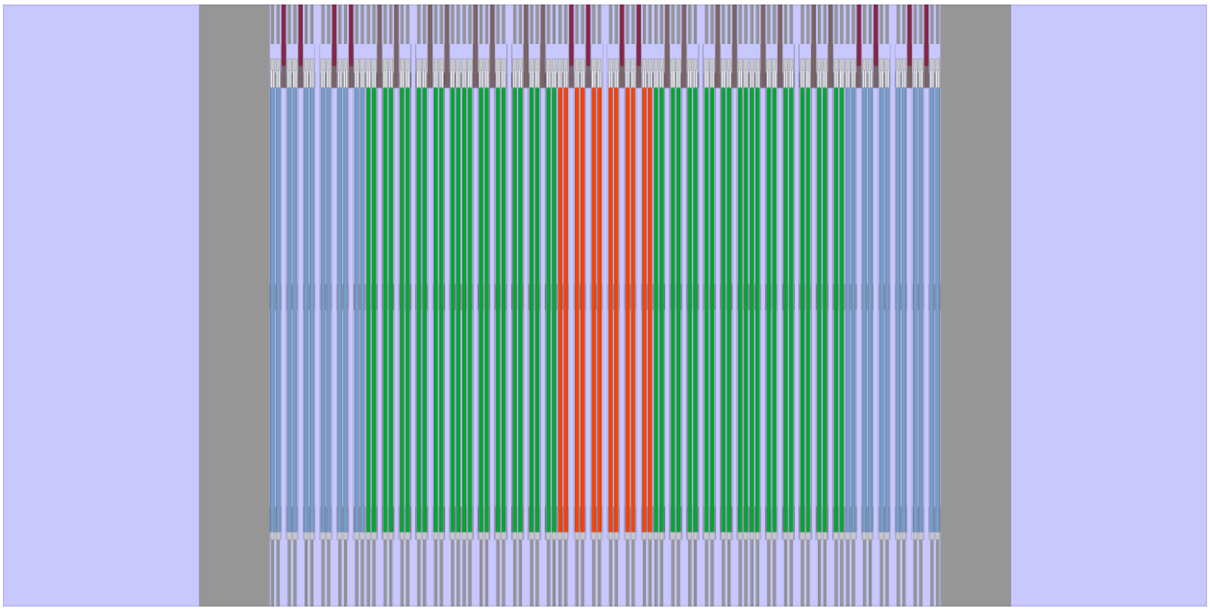

Figure 19. Axial geometry of the core model including the reflector and the downcomer with control rods fully-extracted.

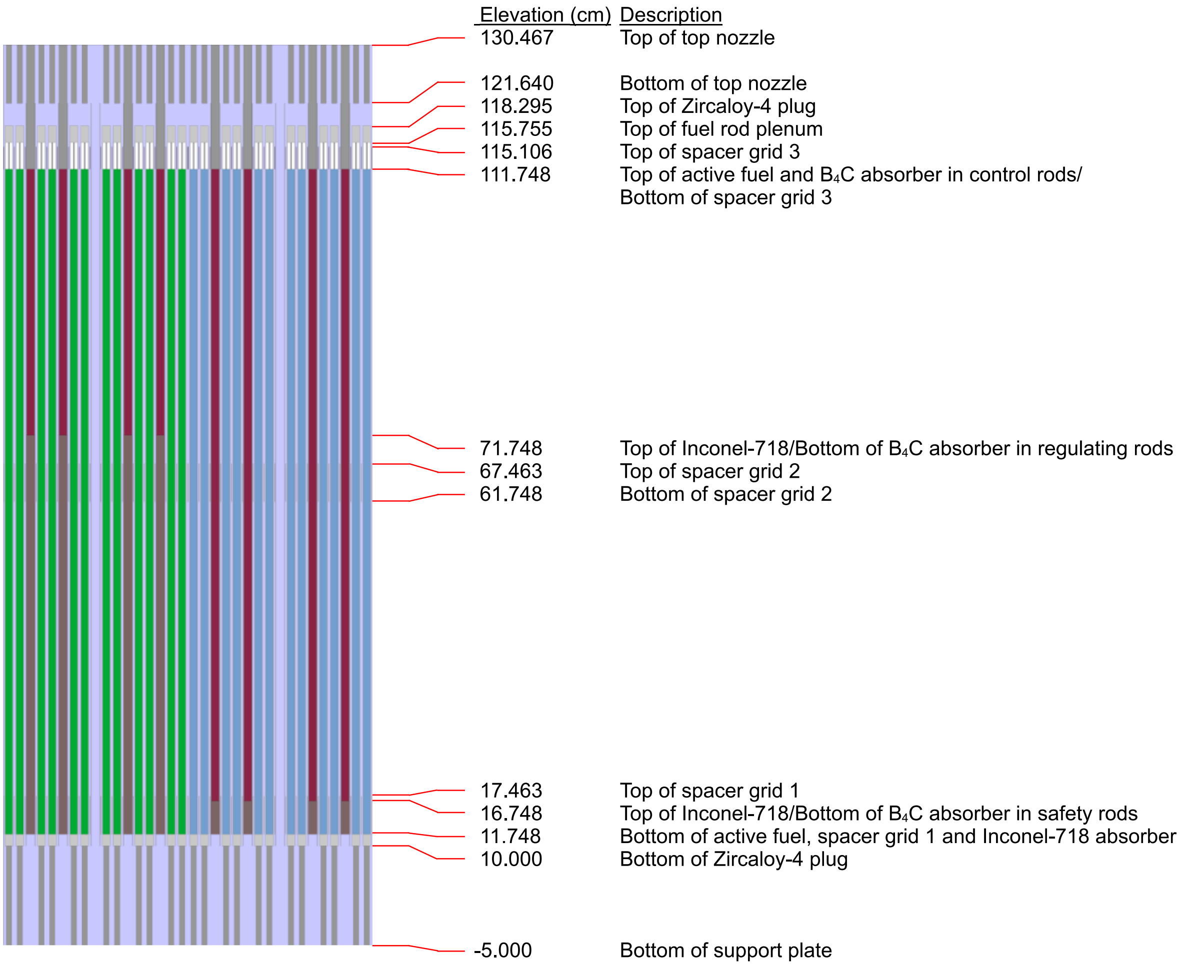

Figure 20. Axial geometry of the model illustrating two fuel assemblies with control rods fully-inserted.

Co-funded by the European Union
UK Research and Innovation
The Research Council of Norway
Project funded by

8.2. Fuel rods

The lattice positions with fuel rods are constructed using the pin cells defined in Section 7.4.1 apart from the region between the upper Zircaloy-4 plug and the top nozzle. In this region a pin cell filled entirely with coolant is used.

8.3. Instrumentation tubes

The instrumentation tube lattice positions are constructed using the empty guide tube/instrumentation tube pin cell (see Section 7.4.2) from the top of the support plate to the bottom of top nozzle. Below and above this region a pin cell filled entirely with coolant is used.

8.4. Guide tubes and control rods

Similarly to the instrumentation tubes, the guide tubes extend from the top of the support plate to the bottom of top nozzle. A guide tube is either filled with coolant or contains a control rod depending on the insertion of the control rods. Pin cell definitions are given in Section 7.4.2. Both regulating and safety rods have two sections: Inconel-718 lower section and 90 % enriched boron carbide upper section. The heights of these sections are 60 / 40 cm for the regulating rods and 5 / 95 cm for the safety rods. The bottom of the Inconel-718 sections of the control rods coincides with the bottom of the active fuel region when the rods are fully-inserted and with the top of the active fuel region when the rods are fully-extracted. Control rods are defined with steel pins above the active absorber regions. As seen in Figure 20 the control rods pass though the top nozzle.

8.5. Spacer grids

The axial locations of the spacer grids are given in Table 3.

Table 3. Spacer grid locations.

Description	Elevation (cm)
SG3 top	115.106
SG3 bottom	111.748
SG2 top	67.463
SG2 bottom	61.748
SG1 top	17.463
SG1 bottom	11.748

9. Material compositions

Material compositions for the core model are tabulated in Appendix 14.1.

Co-funded by the European Union
UK Research and Innovation
The Research Council of Norway
Project funded by

10. Core level boundary conditions

At cold zero power, all materials are at 300 K. At hot full power, core level boundary conditions specified in Table 4 are used. Fuel behaviour can be modelled either in a simplified manner by using the fixed thermophysical properties given in Table 5 or more accurately by utilizing the parameters given in Table 6 with the models/correlations available in the solver being used.

Table 4. Boundary conditions at hot full power.

Parameter	Value	Unit	Note
Power	50	MW	
Core inlet mass flow rate	237.12	kg/s	Uniformly distributed to all fuel assemblies.
Core inlet temperature	379	K	
Core outlet pressure	0.755	MPa	

Table 5. Fixed thermophysical properties for fuel[1] and cladding.

Parameter	Value	Unit
Fuel density	10.295	g/cm^3
Fuel thermal conductivity	5.2	W/(m·K)
Fuel specific heat capacity	290	J/(kg·K)
Cladding density	6.55	g/cm^3
Cladding thermal conductivity	14.7	W/(m·K)
Cladding specific heat capacity	310	J/(kg·K)
Gap conductance	5000	$W/(m^2·K)$

Table 6. Parameters for fuel behaviour modelling.

Parameter	Value	Unit
Fractional theoretical density of the fuel pellet	0.951	-
Plenum length	4.007×10^{-2}	m
Fuel pellet roughness	2.0×10^{-6}	m
Cladding roughness	0.5×10^{-6}	m
Cold work	0.5	-
Cladding average oxygen concentration	0.0012	-
As-fabricated fill gas pressure	0.2×10^{6}	Pa
As-fabricated fill gas temperature	300	K
Fill gas composition	He (100 %)	-

[1] Approximate values for fresh fuel with no gadolinia.

Co-funded by the European Union
UK Research and Innovation
The Research Council of Norway
Project funded by

11. Fuel reload pattern for multi-cycle depletion calculations

Fresh type 4 → C1 → E6 → D3 → out
Fresh type 4 → E1 → C6 → D2 → out
Fresh type 5 → B2 → G4 → C5 → out
Fresh type 5 → F2 → D7 → C3 → out
Fresh type 4 → A3 → F5 → B4 → out
Fresh type 4 → G3 → B5 → E4 → out
Fresh type 1 → D4 → out
Fresh type 4 → A5 → F3 → C4 → out
Fresh type 4 → G5 → B3 → F4 → out
Fresh type 5 → B6 → D1 → E5 → out
Fresh type 5 → F6 → A4 → E3 → out
Fresh type 4 → C7 → E2 → D6 → out
Fresh type 4 → E7 → C2 → D5 → out

The same fuel shuffling pattern, listed above, is used after each fuel cycle, starting after the initial fuel cycle and continuing as long as the simulation is continued. Fresh fuel assemblies, of type 4, 5 or 1 are loaded into 13 positions (C1, E1, B2, …) and the assemblies in those positions are moved to other positions (E6, C6, G4, …) and moreover, the assemblies in those positions are moved (to D3, D2, C5, …) whereas the assemblies from those positions are discharged. This constitutes a three batch loading approach, where the central fuel assembly at D4 is the only exception, being replaced after each fuel cycle.

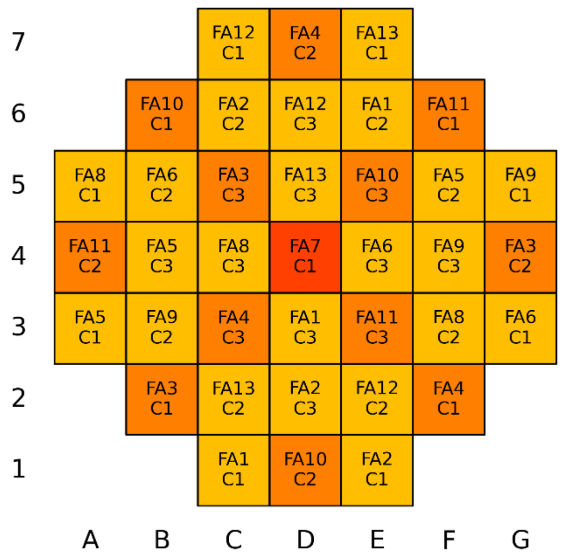

Figure 21: Fuel reload pattern.

All of this information is condensed into the equilibrium core loading pattern presented in Figure 21, where the position of each unique fuel assembly shuffling trajectory (FA1 – FA13) is indicated during each of their three cycles (C1, C2, C3). No rotation is applied to the fuel assemblies when they change positions in the core.

Co-funded by the European Union
UK Research and Innovation
The Research Council of Norway
Project funded by

The equilibrium cycle simulation normally uses the following process, which can be adapted for Subtask 7.5.2 as agreed to among the participants, according to the capabilities of the participating solvers:

1. Start from the fresh initial core (loading pattern Figure 2).
2. Operate reactor at 100 % power (50 MWth) with the full power core level boundary conditions specified for that state.
3. Iterate regulating control rod group positions to obtain a critical reactor with a flat power profile.
4. A control algorithm or an adapted control rod withdrawal order curve can be provided to participants.
5. Deplete system using 5, 10 or 25 day timesteps (25 days ≈ 0.27 MWd/kgU).
6. The first point where regulating groups are fully extracted and the core is subcritical defines the end-of-cycle.
7. The fuel is shuffled using the loading pattern defined in this section and a 21 days decay time is applied.
8. Cycles are simulated until the cycle length and discharge burnups converge (approximately 10 cycles).

12. Conclusions

The data provided in this document should allow the partners to construct the core level models of LDR lite, required as the basis of the analyses in WP7. Geometry and material data were included, along with core level boundary conditions for full power operation and the fuel reload pattern for shuffling between fuel cycles.

13. Bibliography

Horelik, N., Herman, B., Forget, B., & Smith, K. (2013). Benchmark for Evaluation and Validation of Reactor Simulations (BEAVRS), v1.0.1. Proc. Int. Conf. Mathematics and Computational Methods Applied to Nuc. Sci. & Eng. Sun Valley, Idaho.

Komu, R., & Tuominen, R. (2025). LDR lite benchmark specifications, LDR-PUB-VTT-10002-R4. VTT Technical Research Centre of Finland Ltd.

14. Appendices

14.1. Material compositions

Table 7: Material composition, fuel with burnable absorber.

Density (g/cm^3)	1.02950E+01			
U-235 wt-% / Gd_2O_3 wt-%	1.5 / 6.0	1.8 / 6.0	2.4 / 5.0	2.4 / 9.0
Nuclide	Atom density (atom/(b*cm))			
U-234	2.63401E-05	3.16079E-05	4.25918E-05	4.07985E-05
U-235	3.27846E-04	3.93413E-04	5.30126E-04	5.07805E-04
U-238	2.12307E-02	2.11607E-02	2.12443E-02	2.03498E-02
O-16	4.62484E-02	4.62500E-02	4.61995E-02	4.64146E-02
Gd-152	4.10474E-06	4.10474E-06	3.42062E-06	6.15711E-06
Gd-154	4.47417E-05	4.47417E-05	3.72847E-05	6.71125E-05
Gd-155	3.03751E-04	3.03751E-04	2.53126E-04	4.55627E-04
Gd-156	4.20121E-04	4.20121E-04	3.50101E-04	6.30182E-04
Gd-157	3.21196E-04	3.21196E-04	2.67664E-04	4.81795E-04
Gd-158	5.09808E-04	5.09808E-04	4.24840E-04	7.64712E-04
Gd-160	4.48650E-04	4.48650E-04	3.73875E-04	6.72974E-04

Table 8: Material composition, fuel without burnable absorber.

Density (g/cm^3)	1.02950E+01			
U-235 wt-%	1.4	1.5	1.8	2.4
Nuclide	Atom density (atom/(b*cm))			
U-234	2.61533E-05	2.80214E-05	3.36255E-05	4.48335E-05
U-235	3.25521E-04	3.48772E-04	4.18525E-04	5.58027E-04
U-238	2.26107E-02	2.25859E-02	2.25114E-02	2.23624E-02
O-16	4.59248E-02	4.59253E-02	4.59271E-02	4.59305E-02

Table 9: Material composition, fuel rod fill gas (helium).

Density (g/cm^3)	1.59810E-03
Nuclide	Atom density (atom/(b*cm))
He-3	4.80890E-10
He-4	2.40440E-04

Table 10: Material composition, Zircaloy-4.

Density (g/cm^3)	6.54998E+00

Co-funded by the European Union
UK Research and Innovation
The Research Council of Norway
Project funded by

Nuclide	Atom density (atom/(b*cm))
O-16	3.07430E-04
O-17	1.17110E-07
Cr-50	3.29620E-06
Cr-52	6.35640E-05
Cr-53	7.20760E-06
Cr-54	1.79410E-06
Fe-54	8.66990E-06
Fe-56	1.36100E-04
Fe-57	3.14310E-06
Fe-58	4.18290E-07
Zr-90	2.18270E-02
Zr-91	4.76000E-03
Zr-92	7.27580E-03
Zr-94	7.37340E-03
Zr-96	1.18790E-03
Sn-112	4.67350E-06
Sn-114	3.17990E-06
Sn-115	1.63810E-06
Sn-116	7.00550E-05
Sn-117	3.70030E-05
Sn-118	1.16690E-04
Sn-119	4.13870E-05
Sn-120	1.56970E-04
Sn-122	2.23080E-05
Sn-124	2.78970E-05

Table 11: Material composition, stainless steel 304.

Density (g/cm^3)	8.00000E+00
Nuclide	Atom density (atom/(b*cm))
C	1.60571E-04
Si-28	7.90951E-04
Si-29	4.01809E-05
Si-30	2.65192E-05
P-31	3.57736E-05

Co-funded by the European Union
UK Research and Innovation
The Research Council of Norway
Project funded by

S-32	2.14077E-05
S-33	1.69026E-07
S-34	9.57813E-07
S-36	2.25368E-09
Cr-50	7.64894E-04
Cr-52	1.47502E-02
Cr-53	1.67256E-03
Cr-54	4.16335E-04
Mn-55	8.76912E-04
Fe-54	3.53833E-03
Fe-56	5.55443E-02
Fe-57	1.28276E-03
Fe-58	1.70711E-04
Ni-58	5.16868E-03
Ni-60	1.99098E-03
Ni-61	8.65460E-05
Ni-62	2.75949E-04
Ni-64	7.02755E-05

Table 12: Material composition, water at 300 K.

Density (g/cm^3)	9.96560E-01
Nuclide	Atom density (atom/(b*cm))
H-1	6.66172E-02
H-2	7.66186E-06
O-16	3.33124E-02

Table 13: Material composition, isotope enriched boron carbide.

Density (g/cm^3)	2.52000E+00
Nuclide	Atom density (atom/(b*cm))
C	2.74893E-02
B-10	1.06751E-01
B-11	1.07878E-02

Table 14: Material composition, Inconel-718.

Density (g/cm^3)	8.19000E+00
Nuclide	Atom density (atom/(b*cm))
C	3.00006E-04
B-10	4.53924E-06
B-11	1.82711E-05
Al-27	9.13968E-04
Si-28	5.14997E-04
Si-29	2.61622E-05

Co-funded by the European Union
UK Research and Innovation
The Research Council of Norway
Project funded by

Si-30	1.72669E-05
P-31	2.22926E-05
S-32	2.04552E-05
S-33	1.61506E-07
S-34	9.15200E-07
S-36	2.15341E-09
Ti-46	7.65049E-05
Ti-47	6.89942E-05
Ti-48	6.83630E-04
Ti-49	5.01687E-05
Ti-50	4.80359E-05
Cr-50	7.83068E-04
Cr-52	1.51007E-02
Cr-53	1.71230E-03
Cr-54	4.26227E-04
Mn-55	2.85484E-04
Fe-54	8.77557E-04
Fe-56	1.37758E-02
Fe-57	3.18143E-04
Fe-58	4.23389E-05
Co-59	7.61569E-04
Ni-58	3.00327E-02
Ni-60	1.15686E-02
Ni-61	5.02878E-04
Ni-62	1.60341E-03
Ni-64	4.08338E-04
Cu-63	1.46519E-04
Cu-65	6.53667E-05
Nb-93	2.72076E-03
Mo-92	2.31589E-04
Mo-94	1.44724E-04
Mo-95	2.49308E-04
Mo-96	2.61538E-04
Mo-97	1.49898E-04
Mo-98	3.79293E-04
Mo-100	1.51623E-04